

Cryogenic source of atomic tritium for neutrino-mass measurements and precision spectroscopy

A. Semakin, J. Ahokas, T. Kiilerich, and S. Vasiliev

Department of Physics and Astronomy, University of Turku, 20014, Turku, Finland

F. Nez and P. Yzombard

Laboratoire Kastler Brossel, Sorbonne Université, CNRS,

ENS-PSL Université, Collège de France, Paris, France

V.V. Nesvizhevsky

Institut Max von Laue - Paul Langevin, 71 avenue des Martyrs, Grenoble, France

E. Widmann

Marietta Blau Institute for Particle Physics, Austrian Academy of Sciences, Vienna, Austria

P. Crivelli

Institute for Particle Physics and Astrophysics, ETH, Zurich, Switzerland

C. Rodenbeck, M. Röllig, and M. Schlösser

Institute for Astroparticle Physics (IAP), Karlsruhe Institute of Technology (KIT), Eggenstein-Leopoldshafen, Germany.

We propose a concept for a cryogenic source of atomic tritium at sub-Kelvin temperatures and energies suitable for magnetic trapping. The source is based on the dissociation of solid molecular T_2 films below 1 K by electrons from a pulsed RF discharge, a technique recently demonstrated for atomic hydrogen, combined with buffer-gas cooling and magnetic confinement. We analyze the key processes limiting the source performance, adsorption, spin exchange and recombination, and show that atomic tritium fluxes exceeding 10^{15} s^{-1} at kinetic energies of $\sim 100 \text{ mK}$ can be achieved at the entrance to the magnetic trap. Such a source would enable Doppler-free two-photon 1S–2S spectroscopy in atomic tritium for high-precision measurements of the triton charge radius, providing a crucial benchmark for bound-state QED and improving the comparison between electronic, muonic, and scattering determinations of nuclear sizes in light systems. Beyond spectroscopy, an atomic tritium source avoids molecular final-state broadening in the β -decay and is therefore necessary for next-generation neutrino-mass measurements; combined with detector technologies such as sub-eV resolution quantum sensors or cyclotron radiation emission spectroscopy, it enables an order-of-magnitude improvement compared to the current best experimental limit. Additionally, the source can be used to generate a beam of low-field-seeking deuterium atoms for loading magnetic traps, an important benchmark before trapping tritium atoms, which is useful for precision spectroscopy.

I. INTRODUCTION

Studies of atomic hydrogen have played a central role in the development of modern physics. Due to its simplicity, many of its properties can be calculated from the first principles with extremely high accuracy, providing stringent tests of bound-state quantum electrodynamics (QED) [1]. The experimental possibility of reaching Bose–Einstein condensation stimulated extensive research on ultracold hydrogen atoms confined by superfluid helium films [2] or magnetic traps [3], where BEC was finally achieved in 1998 [4]. Renewed interest in such systems has recently emerged in connection with precision spectroscopy [5–7], gravitational quantum states [8, 9], and comparisons with antihydrogen to test the equivalence principle [10–12]. Extending these studies to the heavier isotopes, deuterium and tritium, remains a major challenge, because of their stronger adsorption on helium surfaces and faster recombination. In the case of tritium, precision spectroscopy of the transi-

tion 1S–2S would allow an accurate determination of the triton charge radius, providing an essential benchmark for few-body QED and consistency between the radii obtained from electronic, muonic, and scattering data [13]. Such measurements would also contribute to the resolution of persistent discrepancies among light-nuclear charge radii, which remain despite of recent convergence of some proton-radius determinations [14].

Tritium is of particular interest because it is radioactive and decays by β -emission into ${}^3\text{He}$, an electron, and an antineutrino. Accurate measurements of the electron energy near the endpoint provide a direct determination of the effective electron-neutrino mass. This approach is pursued by several international collaborations, including the Karlsruhe Tritium Neutrino Experiment (KATRIN) [15], Project 8 [16], QTNM [17] and PTOLEMY [18]. The KATRIN experiment, which employs a windowless molecular source of T_2 at 80 K, has recently established an upper limit of 0.45 eV for the neutrino mass, with a projected sensitivity of 0.3 eV (both

at 90% confidence level) in the final stage of its current measurement campaign [19]. These values remain above the expected lower bound of about 50 meV (9 meV) in the case of an inverted mass hierarchy (normal hierarchy). The normal and inverted hierarchies denote the two possible orderings of the neutrino mass eigenstates m_1 , m_2 , and m_3 consistent with oscillation data. In the normal (inverted) ordering one has $m_1 < m_2 < m_3$ ($m_3 < m_1 < m_2$), implying different minimal values for the effective electron-neutrino mass accessible to direct kinematic searches [20]. One of the main limitations of the molecular approach is that part of the β -decay energy is distributed into the ro-vibrational excitations of the final state of T_2 , which broadens the endpoint spectrum [21]. This has motivated the development of sources of *atomic* tritium, where such molecular effects are absent, offering the possibility of reaching much higher precision in future direct neutrino-mass measurements.

Techniques realized for magnetic trapping of H are now considered for holding large amounts of atomic D and T at temperatures $\lesssim 100$ mK. Loading such a magnetic trap requires an efficient source of atoms with energies low enough for trapping with existing superconductive magnet technologies. The dissociation of molecular H_2 , D_2 and T_2 can be carried out in RF discharge [22], by thermal cracking [23] or with a pulsed DC discharge combined with supersonic expansion [24]. Although large fluxes and high degree of dissociation can be achieved with these methods, resulting atoms have very large energy and reducing it to the trappable values is a very difficult task.

In this work, we propose a concept of a cryogenic source of atomic tritium. Dissociating T_2 will be done below 1 K in a thin solid layer inside a dissociator chamber in a pulsed RF discharge similar to what is used to dissociate H_2 [25]. Electrons generated in tritium β -decay at a mean energy of 5.7 keV propagate inside the solid layer and thus provide additional dissociation increasing the total atomic flux. For the H source, following dissociation, the thermalization of the atoms usually takes place through collisions with the cold walls. However, this will not be feasible for tritium. Therefore, buffer gas cooling with ^4He or ^3He vapor combined with radial magnetic confinement is proposed in this work. This method was utilized to cool and trap several atomic and molecular species after laser ablation from the solid target in J. Doyle's group (see [26] for a review). We evaluate that atomic fluxes of the order of 10^{15} T atoms s^{-1} can be obtained at gas temperature of ≈ 0.4 (0.2) K using ^4He (^3He) inside the gas transport tube.

II. PROPERTIES OF H, D AND T

Since the pioneering experiment of Silvera and Walraven in 1980 [2] in which spin-polarized H gas ($H\downarrow$) was stabilized in a container lined with a superfluid helium film, a decade of intensive research was devoted to the

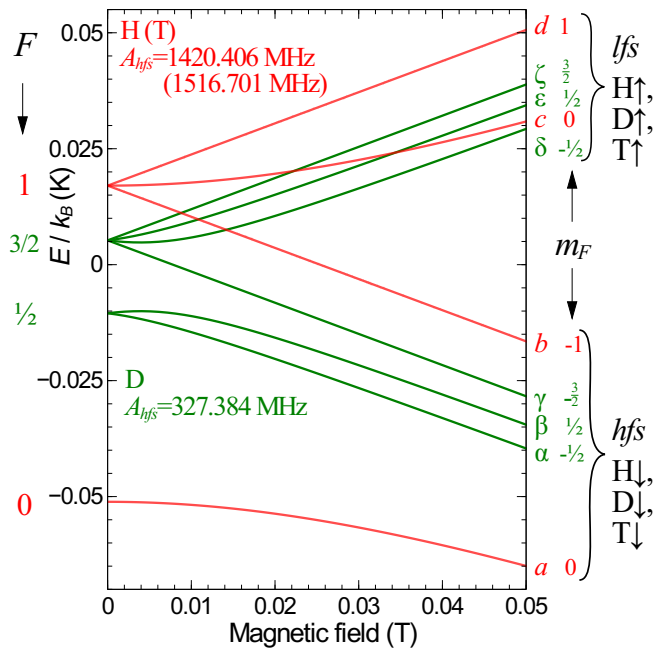


Figure 1. Hyperfine level diagram for H (red) and D (green) and spin states in the low field basis. For T, the diagram is nearly identical to that of H except for the slightly larger value of the hyperfine constant.

experiments with high-field-seeking (*hfs*) atoms ($H\downarrow$) stabilized in strong magnetic fields (see the hyperfine level diagram in Fig. 1). The interaction with helium films was well understood and finally it became clear that the adsorption of the gas on the walls is the main obstacle and that further progress towards BEC requires wall-free confinement in magnetic traps. Finally, BEC was reached at MIT in 1998 [4] by evaporative cooling of low-field seeking (*lfs*) atoms ($H\uparrow$) to ≈ 50 μK in a magnetic trap. Although the atoms were trapped and cooled without contact with the material walls, a superfluid ^4He coverage was needed to provide a cold H beam with a sufficiently low temperature down to 100-200 mK for loading the trap.

Using techniques similar to those with H, several experiments succeeded in stabilizing atomic D inside a container lined with a superfluid helium film in zero [27, 28] and strong magnetic fields [29, 30]. The densities and holding times achieved were substantially lower than those for H. The loading of atomic D into a magnetic trap was not successful [31]. The only experimental work with atomic T was performed by Tjukanov in zero magnetic field [32]. Small densities of gaseous T were detected by the hyperfine resonance at temperatures greater than 8 K. However, no measurable signal below that was observed, even at around 1 K when the surfaces were coated with superfluid helium. Working with D and T turned out to be much more difficult. The reasons for this are related to the stronger interaction with the helium covered wall and faster recombination and relaxation, which

we review below.

A. Interaction with the walls covered by a superfluid helium film

Finding surfaces that would be most suitable for the confinement of atomic hydrogen was a key issue at the early stage of experimental work with cold H \downarrow gas. Liquid helium, due to its smallest density and the formation of a superfluid film below 1 K, turned out to be the only choice to stabilize H \downarrow and D \downarrow [2, 29]. The adsorption energy (E_a) of H on films of a pure mixture of ^4He and ^3He - ^4He has been measured in numerous experiments through studies of a two-body recombination in the adsorbed phase (see [33] and references therein) and by direct measurement of the surface and bulk densities using high field ESR [34]. We present a summary of the experimental data and theoretical predictions of the main properties characterizing the interaction of hydrogen and its isotopes with the helium films of ^4He and ^3He in Table I.

The adsorption energy determines a relation between the surface density σ in the bound state and the bulk gas density above the surface n via the adsorption isotherm:

$$\sigma = n\Lambda_{th}e^{\frac{E_a}{T}}, \quad (1)$$

where Λ_{th} is the thermal de Broglie wavelength.

The adsorption energy for H on the ^4He film is measured with the best accuracy $E_a = 1.14(1)$ K [33] and it can be seen that the surface coverage increases exponentially below 1 K. This sets a limit for the experimentally accessible temperature range down to 100 mK below which surface recombination leads to a very large loss of atoms. In the ^3He - ^4He mixture films at temperatures below 200-300 mK, ^3He also fills the surface-bound (Andreev) states [35]. This leads to a substantial decrease in the adsorption energy of H on such mixture films down to 0.36 K [33]. Due to a larger mass, D has a stronger interaction with the helium film, and the adsorption energy increases over 3 K on ^4He [36]. This limits the lowest experimental temperatures to around 300 mK provided that the recombination rate constant would remain the same, which is actually not the case, as we shall see in the following. To our knowledge, there are no experimental values for the adsorption energy of T. Following the trend between H and D and theoretical estimates, one may expect that it lies between 4 and 5 K for ^4He and 1.5-2.5 K for films ^3He .

Some chance remains that ^3He - ^4He mixture films reduce E_a for tritium, as observed for hydrogen. At small concentrations of ^3He , where the solvation energy may remain roughly the same, the adsorption energy can decrease by a factor of 3, leaving the possibility of experiments in a range between 0.3 and 0.7 K where the adsorbed phase density is not very large while the solvation

probability is still low. To the best of our knowledge, such experiments were not attempted.

B. Surface recombination

Recombination of two hydrogen atoms to a molecule releases ≈ 52000 K of energy, being the main obstacle in experiments with hydrogen atoms at low temperatures. This process requires a third body, which can be another atom or a surface. Three-body processes that occur in the bulk gas or on the surface at very high densities are not considered in this work. Therefore, the two-body recombination on the surface of helium films is the main loss mechanism if the atoms are allowed to collide with the surface, as in experiments with the high-field-seeking atomic states. The surface recombination rate is proportional to the collision rate of the atoms and to the effective cross-section of the recombination which describes the probability of recombination in the collision. The corresponding rate constant can be expressed as $K = \bar{v}l_{rec}$ where $\bar{v} = \sqrt{\pi k_B T/m}$ is the average thermal velocity in 2D, and l_{rec} is the recombination cross-length which may depend on temperature and magnetic field as well as on the hyperfine states of colliding atoms [43]. The atoms in the so-called "pure" high-field seeking hyperfine states b ($F = 1$, $m_F = -1$) for H and T and γ ($F = 3/2$, $m_F = -3/2$) for D (see Fig. 1) cannot recombine in two-body collisions. Therefore, the gas consisting of such states is extremely stable with respect to recombination until three-body processes start to play a role. At low densities, such doubly polarized gas decays via the first- and second-order processes of nuclear relaxation on the surface. For H, all rate surface recombination processes are well established and rate constants are accurately measured [43].

The situation with the surface recombination for D and T is much less understood. Few experiments that attempted to work with D reported much faster recombination rates than those for H with maximum-obtained bulk densities at least an order of magnitude lower. These high rates could not be explained by the factor of 2.5-3 increase in the adsorption energy (see Table I). Discussions in refs. [28, 36] considered a complicated behavior of the effective recombination cross-length dependent on the magnetic field and temperature, as well as the possibility of resonant recombination at certain values of B (Feshbach resonances). For the case of deuterium, the recombination cross-length can exceed the value for H by 2-3 orders of magnitude for a certain B and T . For T, the only experimental attempt [32] did not succeed in stabilizing the T gas below 1 K. Solvation in the helium film and a large recombination cross-section were proposed for the possible explanation. In conclusion, the superfluid helium film coverage, which successfully prevents surface recombination in the H gas, works poorly for D and most likely will not work for T [41].

Isotope	E_a on ^4He	E_a on ^3He	E_s in ^4He	l_{rec} , Å
H theor	0.85 [37], 1.00 [38]	0.36 [37]	36 [39, 40]	
H exp	1.14(1) [33]	0.39(1) [33]		0.4(1) [33]
D theor	2.2 [37], 2.54 [38]	1.2 [37]	14 [39], 15[40]	
D exp	3.1(2) [36]		13.6(6) [41]	<30 [27], >300 [42]
T theor	3.2 [37], 4.77 [38]	1.9 [37]	6 [39], 7.2 [40]	
T exp				>10000 [32]

Table I. A literature compilation of the data for adsorption E_a and solvation E_s energies (in K) along with the recombination cross-length l_{rec} for different hydrogen isotopes.

C. Scattering of H isotopes on each other and on He

Elastic collisions that do not change the spin state of colliding atoms lead to the recovery of thermal equilibrium and are essential for evaporative cooling. Inelastic rates typically lead to a change of the hyperfine state which may lead to the loss of the atoms from magnetic trap as discussed in the next section. Scattering of atoms with helium vapor is important for the transport of hydrogen isotopes into the trapping cell and defines the efficiency of buffer gas cooling, which is one of the key effects in this proposal.

In the zero temperature limit, the elastic collision cross-section σ_{el} is related to the s-wave scattering length a_s as $\sigma_{el} = g_2 4\pi a_s^2$, where g_2 is the two-body correlator defined by quantum statistics and identical properties of colliding particles. $g_2 = 1, 2, 0$ for two distinguishable particles, for two indistinguishable bosons, and for two identical fermions accordingly. The value and sign of the scattering length depend on the interaction potential and the electron spin state of the atoms of the pair. The singlet potential supports a large number of bound molecular states and is not relevant for spin-polarized or spinless atoms considered here. The repulsive triplet potential has a weak well because of the Van-der-Waals attraction and may support weakly bound states, or dimers. The shape of the potential is nearly the same for all atomic pairs considered here. The reduced mass m of the atomic pair turns out to be an important parameter in the scattering properties. The dimer bound state occurs for the heaviest pair considered here ^4He - ^4He pair. The pair of T atoms is very close to the binding resonance [44]. At the scattering resonance, the scattering length diverges and changes sign, going from $-\infty$ to $+\infty$. The scattering length and the collisional cross-section then depend on how far the reduced mass is from the resonance value of ≈ 3.3 [44]. Scattering lengths and cross-sections for elastic collisions of various pairs of H and He isotopes in the zero temperature limit were calculated by several authors [37, 45–47]. We present a summary of the data in Table II. Of particular significance for this work is a very large elastic collision cross-section for the heaviest pairs considered, and especially for the T-T and T-He collisions [44, 47].

Processes that occur in inelastic collisions are the spin-exchange and dipolar relaxation. The first class concerns the collisions of atoms in different or mixed hyperfine states (c for H/T and δ and ϵ for D, see Fig. 1). This process is very important during loading and at the initial stage of magnetic trapping. The exchange and dipolar relaxation rates for numerous channels for atomic hydrogen were calculated in Refs. [44, 48] and experimentally confirmed in the work of the MIT [49, 50] and Amsterdam groups [51].

The situation is very different for fermionic D \uparrow . Due to the Pauli principle, identical D atoms avoid approaching each other, and s-wave scattering is forbidden. For D, theory predicts two orders of magnitude faster spin-exchange rates, and the dipolar relaxation decreasing linearly with temperature as $G_{\zeta\zeta} \approx 10^{-14} \cdot T \text{ cm}^3/\text{s K}$ [52]. Remarkably, the doubly polarized D gas is becoming more stable at lower temperatures, and its decay time at 1 mK is two orders of magnitude larger than that for H, while the thermalization rate remains fairly large [52]. For tritium, relaxation rate constant data were recently calculated [44]. Spin-exchange and dipolar relaxation are much larger than for H, and the rates have a complex dependence on temperature and magnetic field. Under optimal conditions of magnetic fields below 0.01-0.02 T and a temperature of 100 mK the dipolar relaxation rate is 5 times higher than for H. Unfortunately, this implies that the fluxes of T in loading the trap should be increased by the same factor.

D. Magnetic trapping of H \uparrow , D \uparrow , and T \uparrow

Since surface recombination limits the cooling of H \downarrow states below ~ 100 mK, a wall-free confinement method was proposed by Pritchard [53] and later extended to hydrogen by Hess [54]. It is based on trapping low field seekers (\uparrow) in a potential well created by a magnetic field. Cooling of the trapped gas is performed by evaporation of the atoms, which have enough energy to overcome the trapping barrier and carry away the energy. The remaining gas is thermalized in elastic two-body collisions. Successive trapping and cooling experiments were performed at MIT [49] and the University of Amsterdam [51] reaching BEC in 1998 [4]. Recently, a large magnetic trap for

	D-D [45, 46]	T-T [44]	H-T [46]	T- ³ He [47]	T- ⁴ He [47]	³ He- ³ He [45, 46]	³ He- ⁴ He [45, 46]	⁴ He- ⁴ He [45, 46]
$a_s, \text{Å}$	-4	-42	-0.85	-8.8	-22	-7	-17	-110
$\sigma_{el}, 100 \cdot \text{Å}^2$	2	450	0.09	9.7	61	6.4	36	3200

Table II. S-wave scattering length and elastic collision cross-sections for different hydrogen isotopes and helium atoms in the zero temperature limit. For the fermion pairs we consider the case of distinguishable atoms, e.g. in different hyperfine states. Data for the D-D and helium pairs were calculated in refs. [46] and [45] using somewhat different interaction potentials. The difference for the a_s does not exceed 10% and we present average values. For the temperature dependent cross sections of hydrogen and helium isotope pairs see ref. [47].

H was built and tested in the University of Turku [55]. The typical range of H densities confined in magnetic traps is between 10^{11} and 10^{14} cm^{-3} and minimum temperatures are several tens of μK .

The trappable low field seeking states c ($F = 1$, $m_F = 0$ in zero field basis) and d ($F = 1$, $m_F = 1$) are higher in energy than two other hyperfine states a ($F = 0$, $m_F = 0$) and b ($F = 1$, $m_F = -1$) (see Fig.1). Relaxation to the lower energy states is threshold-less and does not vanish even at zero temperature. Spin exchange during two-body collisions is the fastest loss channel. It occurs in collisions where the "mixed" state c takes part leading to a rapid depletion of the c state in the trap. The remaining "pure" and doubly polarized state d is much more stable since spin-exchange does not work in this case. However, the dipolar interaction during collision of two d atoms may lead to spin flip and relaxation to untrapped states. This channel of dipolar relaxation is the main loss mechanism that limits the lifetime and maximum densities of the trapped gas. This is a second order, in density, process with the characteristic decay time inversely proportional to the gas density. For H, the two-body dipolar relaxation rate constant is $\sim 10^{-15} \text{ cm}^3/\text{s}$ [48], which implies a lifetime of $\sim 10^3 \text{ s}$ at the density $n = 10^{12} \text{ cm}^{-3}$.

Stability of the trapped T gas is basically determined by relaxation processes similar to those in H. Both atoms are bosons and have a similar hyperfine structure. However, the three fold larger mass has a strong effect. As recently calculated [44], the low-energy cross sections for T-T collisions are substantially larger than those for H-H. This concerns both elastic and inelastic collisions. The reason is that a scattering resonance appears in collisions of atoms with a hypothetical mass slightly greater than 3 [44]. Two T atoms are very close to the formation of the bound dimer state. The s-wave scattering length is very large and negative $a_T \approx -43 \text{ Å}$. This increases the elastic collision rate and enhances the efficiency of evaporative cooling. However, inelastic dipole relaxation is increased as well. For the relaxation d - d of two T atoms in a magnetic field of 1 mT and temperature of 1 mK, typical for H trapping, the increase reaches a factor of ≈ 50 compared to that for H-H collisions. The dipolar rate for T-T collisions has a much stronger temperature dependence, and the difference with H decreases to a factor of ≈ 5 for $T=100 \text{ mK}$. This leads to an increase in the loss rate and a decrease in the life-time of the trapped T

gas by the same factors at equal density. To our knowledge, magnetic trapping of T \uparrow has not been attempted to date, and the theoretical predictions above are still waiting for experimental confirmation.

As mentioned in the previous section, trapping of atomic D would allow substantially larger densities and very high stability of the trapped gas [52]. Compared with the potential of all three isotopes for precision spectroscopy in the magnetic traps, deuterium is obviously the best candidate. However, the only attempt to trap the D \uparrow gas performed by the MIT group using the same dissociation and trapping techniques as for H \uparrow [31] was unsuccessful. The walls of their trapping cell were covered with superfluid helium film. Although some flux of D entering the trap was detected, no signal was seen after the dissociator was switched off. The large adsorption energy on the helium film and fast recombination rate on the surface of the trapping cell were proposed as a possible explanation for their failure to load the trap.

E. Stabilization of H, D, and T in solid molecular matrices

Matrix isolation of unstable radicals and atoms is a well-established method in experimental physical chemistry. Unpaired atoms are stabilized in solid inert crystals of H₂, He, Ne, Ar. The main fundamental interest in studies of H and its isotopes in such matrices is related to the possibility of quantum diffusion at ultra-low temperatures, the possibility of observation of superfluidity/supersolidity of impurity atoms.

Several methods are known to produce the matrices with embedded atoms. We briefly describe two methods relevant to this work: dissociation with cryogenic RF discharge and electrons resulting from the β -decay of T₂. The first technique is based on an in-situ dissociation of the matrix molecules using pulsed RF discharge in the helium vapor above solid films of hydrogen below 1 K introduced by Ahokas *et. al.* [56]. The molecules are split by the impact of the electrons of the discharge having energies of the order of 100 eV. It turned out that a fraction of the atoms is evaporated during the RF pulse, and the H and D atoms in a gas phase can be accumulated in the sample cell when its surfaces are covered by a superfluid helium film. The operation of the cryogenic dissociator which we will describe in the

following is based on this effect.

The second dissociation method is based on the natural radioactivity of T, which is mixed into solid films [57, 58]. The dissociation of molecules is caused by the β -decay electrons generated inside the films. Even a few % concentration of T₂ or HT in the sample is sufficient to produce samples with large ($\gtrsim 10^{20} \text{ cm}^{-3}$) concentrations of H and D atoms in various matrices [59].

A detailed study of tritiated solid hydrogen films below 1 K was performed at the University of Turku with direct atom diagnostics using magnetic resonance methods: ESR and ENDOR [59, 60]. T₂ films of 35 and 250 nm thickness were deposited onto the surface of a quartz microbalance (QM) which provided accurate control of the film thickness during deposition and measurements. The QM gold electrode also served as a mirror of the Fabry-Perot resonator connected to an ESR spectrometer operating at 128 GHz. For a film of 250 nm thick, ESR lines of T were detected a few minutes after deposition and grew rapidly, reaching a maximum concentration of $\approx 2 \cdot 10^{20} \text{ cm}^{-3}$ ($\approx 0.5\%$ relative to the density of molecules) after three hours. Then, depending on the storage temperature, periodic heat spikes were observed in the sample cell followed by a 30-40 % decrease in the density of T and $\sim 5\%$ decrease in the thickness of the film. This behavior was explained by an explosive recombination of the atoms in the films after they reached some critical density. The explosions were not observed in a thinner T₂ film of 35 nm thickness and were suppressed by condensing a superfluid helium film on top of the 250 nm T₂ film. The maximum T densities reached during storage decreased by a factor of 1.8 after heating the 250 nm film from 0.1 to 1 K, and the time between explosions has increased by a factor of ~ 2 . Clearly, thermal explosions can be avoided by improving the heat removal from the T₂ film or if the atoms can be removed from the solid matrix (e.g. by running the RF discharge) before a large concentration is accumulated.

III. CRYOGENIC DISSOCIATOR

A. Hydrogen and *hfs* of deuterium

The cryogenic hydrogen dissociator of H operating below 1 K was first realized in the group of W. Hardy at the University of British Columbia [61, 62]. The method is based on a cryogenic discharge in a helium vapor and is similar to the technique mentioned above and used to produce H atoms inside solid molecular H₂ matrices. The molecules in solid are split by impacts of the electrons of plasma discharge produced during short pulses. Part of atoms evaporate into the bulk of the dissociator chamber and are then pushed by magnetic field gradients out of the dissociator. This technique also allowed to design sources of low field seeking H atoms for loading magnetic traps. The transport of atoms to the trap could be done via a short tube, filling the trap with hot gas of atoms

with subsequent thermalization and isolation from the walls of the trap [49–51] or following several stages of thermalization and cooling them to ~ 100 mK before entering the trap. The latter technique was described in a previous publication of the Turku group [25], where the operation of the cryogenic dissociator for H is described in detail. Atomic fluxes close to 10^{14} s^{-1} of *lfs* H are obtained by this technique and were successfully used to load a large magnetic trap [25].

It is useful to consider what happens with the helium film and its vapor in the cryogenic dissociator during and after the RF discharge pulse. In a typical operation with H [25], the discharge is driven by RF pulses of ~ 1 ms length followed by ~ 20 ms OFF time. The RF power is adjusted to the maximum value, which the dilution refrigerator can tolerate but is lower than the threshold for full evaporation of the helium film inside the dissociator chamber. The energy released in the dissociator resonator during the 1 ms RF pulse is sufficient to evaporate $\approx 3 \cdot 10^{-7}$ moles of ⁴He which has ≈ 70 J/mole latent heat of evaporation at 0.6 K [63]. This is nearly half of the total amount of helium that covers the walls of the dissociator. During the dissociator operation, its average temperature increases from 0.6 to ≈ 0.64 K, leading to an increase in the ⁴He vapor density in the chamber from $4.5 \cdot 10^{15} \text{ cm}^{-3}$ to $1.05 \cdot 10^{16} \text{ cm}^{-3}$ [64, 65]. We used here the average temperatures during pulsed operation measured by a thermometer at the dissociator body. Obviously, the temperature during the pulse is somewhat higher, and therefore the estimate above represents a lower bound for the density of helium vapor during the pulse.

We can estimate the upper limit if we assume that the amount of liquid evaporated during the pulse is instantly converted into vapor. This gives a vapor density of $1.4 \cdot 10^{16} \text{ cm}^{-3}$, quite close to the lower bound estimate. However, this vapor during and after the pulse flushes out of the dissociator and is re-condensed in the colder regions of the transfer line. The vapor is dense enough to entrain D(T) atoms that were produced during the discharge pulse, and it pushes them towards the colder regions of the transfer line. This effect, similar to the operation of the old diffusion pump, is useful to increase the efficiency of the atomic source. It was first observed in the first experiments on the stabilization of H \downarrow [2] and received the acronym HEVAC (Helium Vapor Compressor). The superfluid flow along the walls of the transfer line returns helium into the dissociator chamber. Such circulation of helium exists in any system where there is a gradient of temperature and often creates problems because of the associated heat load to the lower temperature parts of the system.

A cryogenic dissociator of this type was also used in experiments with atomic *hfs* of D, for the hyperfine resonance study of an unpolarized gas in a zero field [27, 41] and with two-dimensional D in a strong magnetic field [36]. The fluxes were a factor of 5-10 smaller than for H. Attempts to load the *lfs* to a magnetic trap

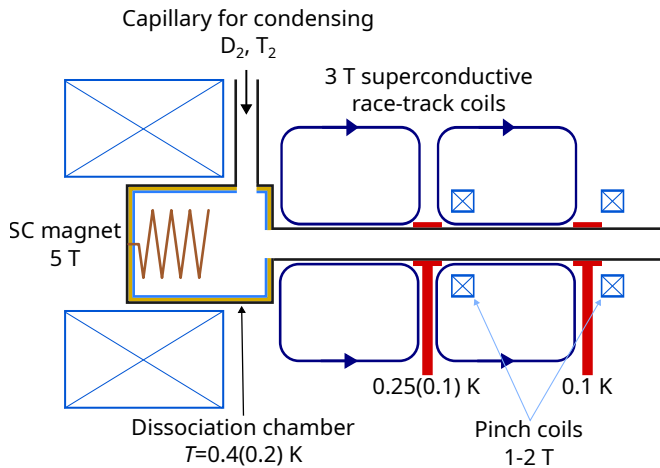


Figure 2. Schematic of the cryogenic source of D and T. Temperatures in the brackets are for the 5% ^3He - ^4He mixture film.

at MIT were unsuccessful [31]. The reason may be in the transfer line between the dissociator and the trapping cell, which was very short. The trap was filled with very warm gas, which recombined at subsequent cooling via thermalization with the walls. Clearly, some improvements are needed for the D source for loading magnetic traps with lfs , which we consider in the next section.

B. Deuterium and tritium lfs

Our proposal for the cryogenic source of lfs D and T is based on the dissociation technique below 1 K described above. However, further cooling of atoms and their transport to the magnetic trap should not rely on thermalization of atoms by collisions with the superfluid helium covered wall of the transfer line. As mentioned above, the latter may work somehow with hfs of D, may not work well with lfs of D, and highly likely will not work with T. However, the presence of helium cannot be avoided in the dissociator chamber. Helium vapor is necessary for running the discharge in the dissociator. All hydrogen isotopes have too low saturated vapor pressures to maintain discharge below 1 K. Therefore, we consider the same construction for the D(T) dissociator: copper chamber with a pre-condensed solid layer of $D_2(T_2)$ on its inner walls and a saturated helium film on top of that. A helical resonator with a resonance frequency in the 100-500 MHz range is located inside; see Fig. 2.

The dissociator chamber is located at the edge of a superconductive magnet with a maximum field of 4-5 T. The magnetic field gradient separates the atoms with opposite electron spins, pushing lfs out into a transfer line. We propose building the transfer line with two sections and thermalization points between, each at slightly lower temperature (see Fig. 2). A system of sextupole or octupole race-track coils with 6 or 8 linear conductors around each of the transfer line sections provides a radial

magnetic field gradient. The fields of 3 T are technically available with modern superconducting technologies for such race-track type of coils. This provides a radial potential barrier of ~ 2 K. For effective isolation of the lfs atoms from the wall, their thermal energies must be 5-10 times lower than the height of the potential barrier, i.e., the atoms leaving the dissociator should be cooled to 0.2-0.4 K. The temperature of the dissociator should be lowered as close as possible to this limit, and the geometry of the transfer line just after it should be optimized for a minimum number of wall collisions.

Lowering the dissociator temperature leads to a very steep decrease in the saturated vapor density of helium in the considered temperature range. In Fig. 3, we present the dependence of the saturated vapor density of ^4He and ^3He as a function of temperature [66, 67]. Since we aim to thermalize the T gas with the helium vapor, we should have a mean-free path for the collisions of T with He comparable to the diameter of the transfer line, which we assume to be ~ 1 cm. Using the temperature-dependent cross sections for the collisions of T with ^4He from ref. [47] we find that the mean-free path for T- ^4He collisions becomes equal to 1 cm at 440 mK.

We can use ^3He - ^4He mixture films to increase the vapor density at a given temperature. Pure ^3He cannot be used because the film will not be superfluid. Mixtures up to $x_3 \sim 5\%$ of ^3He were previously used by the Turku cryogenic dissociator of hfs of H [33]. It is known that the vapor pressure P_3 above a regular solution of ^3He in ^4He is higher than $x_3 \cdot P_3^{sat}$, the product of saturated vapor pressure P_3^{sat} at the same temperature and the concentration x_3 of ^3He in the liquid [68]. The concentration of ^3He in the film inside a tube with a temperature gradient should increase towards the warmer end due to an osmotic effect [68]. Considering that both the above-mentioned effects lead to an enhancement of the ^3He density in the dissociator, we take $x_3 \cdot P_3^{sat}$ as a lower limit estimate for the vapor density above the 5% mixture. Then, we evaluate the minimum dissociator temperature $T \approx 220$ mK for which the T mean free path in the ^3He vapor becomes equal to 1 cm. These temperature estimates match the above-mentioned value for reliable magnetic isolation from walls using 3 T magnets. In the following, two modes of operation for the dissociator are considered: with pure ^4He ($T=0.44$ K) and with 5% ^3He - ^4He mixture ($T=0.22$ K) films.

A small temperature gradient in the transfer line will lead to condensation of helium vapor in the colder regions of the transfer line. The vapor pressure gradient will move the T-He mixture towards the colder region until the vapor density vanishes and the D(T) gas gets decoupled from the walls. For the 5% ^3He - ^4He mixture film, this will happen somewhere in the middle of the second section and the gas will end up cooled to 220 mK or slightly below. With pure ^4He this will occur already in the beginning of the first section and the gas will pass further without cooling.

Efficiency of the buffer gas cooling can be increased

by increasing the length of the atom guide after the dissociator. In the estimates above we set a constraint on the mean-free path of 1 cm. However, the length of the section following the dissociator can be as large as 1 m. Exchange of energy in the elastic collisions of T with helium is very efficient due to the closeness of masses. Each collision reduces the energy difference by the factor of two, and 2-3 collisions are sufficient for good thermalization [26]. In this case, reaching the low temperature end of the atom guiding line, T gas will undergo several collisions at temperatures below 0.2(0.4) K.

The KATRIN++ and Project8 projects plan to use large magnetic traps for storage of T atoms for neutrino mass measurements. In principle, the temperature range of 0.22-0.44 K achieved with the T source described above is already sufficiently low for magnetic trapping. A superconductive trap with 3.1 T (2 K) magnetic barrier has been built in the High Energy Accelerator Research Organization (KEK) Laboratory in Japan [69] and used to trap ultra-cold neutrons [70]. However, for the large trap volumes considered (up to 10 m^3), smaller fields and lower temperatures are preferable. Also, as we discussed in Section II D, the minimal atom loss due to dipolar relaxation is reached at around 0.1 K. In order to increase the efficiency of the buffer gas cooling even under the condition that the mean-free path of T-He collisions is larger than the transfer line diameter, we propose slowing down the flow of the T beam along the line. This can be done by placing extra pinch coils after each section, which will provide potential barriers for the atoms. These coils will provide an impedance for gas flow along the transfer line and increase the number of collisions with the low-density buffer gas. Another option to cool the D(T) gas flowing in the transfer line without buffer gas was recently proposed by the Project 8 collaboration [71, 72]. They propose using evaporative cooling that allows the high-temperature tail of the energy distribution of the flowing gas to overcome the radial magnetic barrier and be removed.

For experiments aiming at precision spectroscopy and the observation of the gravitational quantum states of D or T, we propose feeding the atomic beam out of the cryostat with the dilution refrigerator to room temperature instruments, so that the experiments can be done using the same techniques as is done with a 6 K nozzle [9, 73]. Since the superfluid helium film is supposed to line the inner walls of the transfer line, extending it to room temperature requires suppression of the film and preferably also He vapor flow together with the atomic beam. This can be done by installing a superfluid film cutter based on the evaporation and condensation of the film in a specially designed geometry [65, 74] or by suppressing superfluid flow on the surface coated with Cs [75].

For experiments with slow beams, we may employ the pulsed mode of operation of the dissociator. The average flux of 10^{15} atoms/s considered above consists of pulses 1 ms long followed by a delay of 20 ms. The number of atoms in each pulse is $\approx 2 \cdot 10^{13}$ and close to that

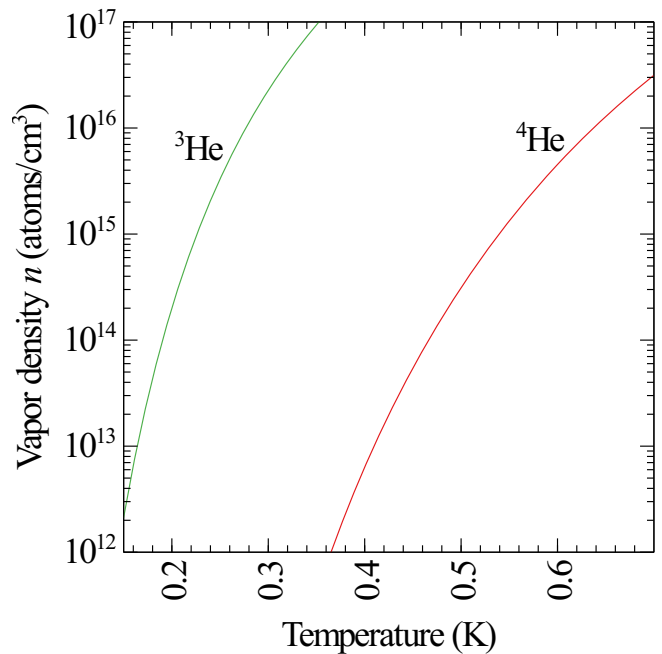


Figure 3. Helium saturated vapor densities as a function of temperature above the liquid. The ^3He curve is based on data from [67], while the ^4He curve is from [66].

reported by Helffrich [76] for a similar type dissociator for H. The D(T) beams at 0.2-0.4 K can be slowed at room temperature using Zeeman decelerators. This technique is based on applying decelerating magnetic field pulses synchronized with the motion of the bunches of atoms in the beam. For H, a device consisting of 12 deceleration stages decreased atom velocities from 520 to 100 m/s [77] with an average deceleration of 35 m/s per stage. Two to three such stages will be enough to completely stop the 0.2-0.4 K cold D (T) atoms exiting from the source proposed in this work.

Technically, cooling the dissociator to 0.2 K can be done by thermally anchoring its chamber to the cold plate of the dilution refrigerator, typically operating at 0.1-0.2 K. Working with pure ^4He requires higher temperatures ~ 0.4 K, which can be obtained by using a ^3He refrigerator and cooling the next stages of the transfer line with a dilution refrigerator. In the Turku lab, a cryogenic system with two refrigerators in one cryostat: dilution and ^3He type, was used for H *hfs* studies. The ^3He refrigerator also has substantially larger cooling power at ~ 0.3 K than the dilution refrigerator cold plate.

One strategy to increase the atom flux from the source is to increase the discharge RF power. As a reference, the H source in Turku is running at an average power of 1 mW as reported previously [25]. The flux of atoms saturated at around this power value, and increasing it further by a factor of 2 stopped the flux completely. As a possible explanation, we consider an insufficient backflow of superfluid film into the dissociator chamber that could not be compensated for by evaporation of helium inside,

leading to the dissociator drying out of the helium film at RF powers exceeding some critical value of ~ 2 mW. This problem can be solved by increasing the diameter of the transfer line and by coating the surface of the inner walls with a sintered layer of copper or silver powder. Then, the maximum dissipated power in the dissociator will be limited by the available cooling power at 0.2 or 0.4 K. In the latter case, using a ^3He refrigerator, it can be $\gtrsim 50$ mW, which may potentially increase the atomic flux by a factor of 50 and reach values well above 10^{15} s^{-1} .

Using ^3He - ^4He films may be challenging when running the dissociator at the highest power of 50 mW. It is known that the transport properties of such films and the critical superflow velocity are reduced due to the presence of ^3He , which contributes to a normal component of the film [78]. In this case, the concentration of ^3He can be reduced to a level required for stable operation of the dissociator; the operation may resume with pure ^4He films.

C. Self-dissociation of T_2 in the dissociator chamber by β -decay electrons.

So far, we have considered that the dissociation of molecules in the solid T_2 layer in the dissociator chamber is performed by the electrons of the RF discharge. As described in Section II E, electrons resulting from the β -decay of T also effectively produce atoms in the solid layer. In the previous work of the Turku group with T in T_2 [60], very thin films of a maximum of 250 nm were used, limited by the exemption limit for work with radioactive materials (1 GBq). We found that each β -electron dissociated about 25 molecules and produced 50 atoms. With a dissociation energy of 4.6 eV, this corresponds to a production efficiency of $\lesssim 0.05\%$. The penetration depth of 5.7 keV electrons in solid hydrogen is about $\sim 3.5 \mu\text{m}$ [79], and we expect that the dissociation number per T decay will be substantially larger for thicker films.

We consider the following design for large flux applications. The cylinder-shaped dissociator chamber with a diameter of 10 cm and a length of 10 cm will be covered inside by a T_2 layer of $1 \mu\text{m}$ thickness. The total amount of T_2 is $\approx 3 \cdot 10^{-3}$ moles and the rate of β -decay events in this layer is $\approx 6 \cdot 10^{12} \text{ s}^{-1}$. Taking the same dissociation efficiency of 50 atoms per T decay, we evaluate the lower bound for the production rate of atoms in solid T_2 as $\dot{N}_T \approx 5 \cdot 10^{14} \text{ s}^{-1}$. If we assume that the

efficiency scales linearly with thickness, then it should increase to 200 events/decay, and the T production rate will be $\sim 2 \cdot 10^{15} \text{ s}^{-1}$. This is larger than the T flux we may get from the dissociator by running the pulsed RF discharge above the solid film with 50 mW power. The heat released by the amount of T in the estimate above is evaluated as ≈ 10 mW, five times smaller than the RF power. The self-dissociation of T_2 seems to be a very efficient mechanism and may provide better efficiency than the RF discharge. As we mentioned in Section II E, the presence of the superfluid helium film improves the cooling of the T_2 films and helps to avoid thermal explosions and partial evaporation of the film. One may try to increase the thickness of T_2 further if the cooling by the helium film will still be able to stop thermal explosions. Finally, both dissociation methods, running the RF discharge on top of the T_2 film, and self-dissociation, will work together, and reaching the flux of atoms above $2 \cdot 10^{15} \text{ s}^{-1}$ seems quite realistic.

IV. CONCLUSIONS

We propose a concept of a cryogenic source of atomic tritium based on a pulsed RF discharge below 1 K, a technique successfully used to produce large fluxes of atomic hydrogen. We expect an extra enhancement of the dissociation rate due to contributions of electrons resulting from the β -decay of T. Working with T requires to prevent the interaction of atoms with the walls where they adsorb and recombine, even if a superfluid helium film is used. We suggest using a buffer gas cooling technique to provide a thermal link between atoms and the walls without physical contact. The atoms are expelled from the walls by magnetic field gradients. Thermal contact via the buffer gas may be easily adjusted by small changes in the temperature distribution in the gas transfer line. Optimal geometry and operating parameters may be found in experimental tests of a source prototype. We evaluate that the fluxes of T atoms exceeding 10^{15} s^{-1} can be reached at temperatures of ~ 100 mK, optimal for magnetic trapping and other experiments with the beams of slow D and T atoms.

V. ACKNOWLEDGMENTS

This project was supported by the Jenny and Antti Wihuri foundation.

-
- [1] U. D. Jentschura and G. S. Adkins, *Quantum Electrodynamics: Atoms, Lasers and Gravity* (World Scientific, 2022).
 [2] I. F. Silvera and J. T. M. Walraven, Stabilization of atomic hydrogen at low temperature, Phys. Rev. Lett.

- 44, 164 (1980).
 [3] T. Greytak, D. Kleppner, D. Fried, T. Killian, L. Willmann, D. Landhuis, and D. Moss, Bose-einstein condensation in atomic hydrogen, Physica B **280**, 20 (2000).

- [4] D. G. Fried, T. C. Killian, L. Willmann, D. Landhuis, S. C. Moss, D. Kleppner, and T. J. Greytak, Bose-Einstein condensation of atomic hydrogen, *Phys. Rev. Lett.* **81**, 3811 (1998).
- [5] A. D. Brandt, S. F. Cooper, C. Rasor, Z. Burkley, A. Matveev, and D. C. Yost, Measurement of the $2S_{1/2} - 8D_{5/2}$ transition in hydrogen, *Phys. Rev. Lett.* **128**, 023001 (2022).
- [6] S. Scheidegger and F. Merkt, Precision-spectroscopic determination of the binding energy of a two-body quantum system: The hydrogen atom and the proton-size puzzle, *Phys. Rev. Lett.* **132**, 113001 (2024).
- [7] M. Amit *et al.*, Towards trapping of hydrogen atoms for computable optical clock applications, *Physical Review A* **112**, 033101 (2025).
- [8] S. Vasiliev, J. Ahokas, J. Järvinen, V. Nesvizhevsky, A. Voronin, F. Nez, and S. Reynaud, Gravitational and matter-wave spectroscopy of atomic hydrogen at ultra-low energies, *Hyperfine Interactions* **240**, 1 (2019).
- [9] C. Killian, P. Blumer, P. Crivelli, O. Hanski, D. Kloppenburg, F. Nez, V. Nesvizhevsky, S. Reynaud, K. Schreiner, M. Simon, S. Vasiliev, E. Widmann, and P. Yzombard, Grasian: towards the first demonstration of gravitational quantum states of atoms with a cryogenic hydrogen beam, *The European Physical Journal D* **77**, 50 (2024).
- [10] M. Ahmadi *et al.*, Characterization of the $1S-2S$ transition in antihydrogen, *Nature* **557**, 71 (2018).
- [11] L. O. A. Azevedo, R. J. S. Costa, W. Wolff, A. N. Oliveira, R. L. Sacramento, D. M. Silveira, and C. L. Cesar, Adaptable platform for trapped cold electrons, hydrogen and lithium anions and cations, *Commun. Phys.* **6**, 112 (2023), arXiv:2301.13248 [physics.atom-ph].
- [12] C. J. Baker *et al.*, Precision spectroscopy of the hyperfine components of the $1S-2S$ transition in antihydrogen, *Nature Phys.* **21**, 201 (2025).
- [13] S. Schmidt *et al.*, The next generation of laser spectroscopy experiments using light muonic atoms, *Journal of Physics: Conference Series* **1138**, 012010 (2018).
- [14] H. Gao and M. Vanderhaeghen, The proton charge radius, *Rev. Mod. Phys.* **94**, 015002 (2022).
- [15] M. Aker *et al.*, The design, construction, and commissioning of the katrin experiment, *Journal of Instrumentation* **16** (08), T08015.
- [16] A. A. Esfahani *et al.*, Determining the neutrino mass with cyclotron radiation emission spectroscopy—project 8, *Journal of Physics G: Nuclear and Particle Physics* **44**, 054004 (2017).
- [17] A. A. S. Amad *et al.*, Determining absolute neutrino mass using quantum technologies, *New Journal of Physics* **27**, 105006 (2025).
- [18] M. Betti *et al.*, Neutrino physics with the ptolemy project: active neutrino properties and the light sterile case, *Journal of Cosmology and Astroparticle Physics* **2019**, 047.
- [19] M. Aker *et al.*, Direct neutrino-mass measurement based on 259 days of KATRIN data, *Science* **388**, 180 (2025), <https://www.science.org/doi/pdf/10.1126/science.adq9592>.
- [20] I. Esteban, M. C. Gonzalez-Garcia, M. Maltoni, I. Martinez-Soler, J. P. Pinheiro, and T. Schwetz, NuFit-6.0: updated global analysis of three-flavor neutrino oscillations, *J. High Energ. Phys.* **2024**, 216.
- [21] L. I. Bodine, D. S. Parno, and R. G. H. Robertson, Assessment of molecular effects on neutrino mass measurements from tritium β decay, *Phys. Rev. C* **91**, 035505 (2015).
- [22] J. T. M. Walraven and I. F. Silvera, Helium-temperature beam source of atomic hydrogen, *Review of Scientific Instruments* **53**, 1167 (1982).
- [23] K. G. Tschersich, J. P. Fleischhauer, and H. Schuler, Design and characterization of a thermal hydrogen atom source, *Journal of Applied Physics* **104**, 034908 (2008).
- [24] S. Scheidegger *et al.*, Barrier-discharge source of cold hydrogen atoms in supersonic beams: Stark effect in the $1S-2S$ transition, *Journal of Physics B: Atomic, Molecular and Optical Physics* **55**, 155002 (2022).
- [25] A. Semakin, J. Ahokas, O. Hanski, S. Dvornichenko, T. Kiilerich, F. Nez, P. Yzombard, V. Nesvizhevsky, E. Widmann, P. Crivelli, *et al.*, Cold source of atomic hydrogen for loading large magnetic traps, *EPJD* **79**, 23 (2025).
- [26] N. R. Hutzler, H.-I. Lu, and J. M. Doyle, The buffer gas beam: An intense, cold, and slow source for atoms and molecules, *Chem. Rev.* **112**, 4803 (2012).
- [27] M. E. Hayden and W. N. Hardy, Atomic hydrogen-deuterium mixtures at 1 kelvin: Recombination rates, spin-exchange cross sections, and solvation energies, *J. Low Temp. Phys.* **99**, 787 (1995).
- [28] T. Arai, M. Yamane, A. Fukuda, and T. Mizusaki, The second order recombination and spin-exchange relaxation of atomic deuterium at low temperatures in a low magnetic field, *J. Low Temp. Phys.* **112**, 373 (1998).
- [29] I. F. Silvera and J. T. M. Walraven, Spin-polarised atomic deuterium: Stabilization, limitations on density, and adsorption energy on helium, *Phys. Rev. Lett.* **45**, 1268 (1980).
- [30] I. Shinkoda, M. W. Reynolds, R. W. Cline, and W. N. Hardy, Observation of doubly spin-polarized deuterium by electron-spin resonance, *Phys. Rev. Lett.* **57**, 1243 (1986).
- [31] J. K. Steinberger, *PhD. Thesis: Progress Towards High Precision Measurements on Ultracold Metastable Hydrogen and Trapping Deuterium*, Ph.D. thesis, MIT (2004).
- [32] E. Tjukanoff, P. Souers, and W. N. Hardy, Zero-field magnetic resonance studies of atomic tritium (World Scientific, 1988) p. 105.
- [33] A. I. Safonov, S. A. Vasilyev, A. A. Kharitonov, S. T. Boldarev, I. I. Lukashevich, and S. Jaakkola, Adsorption and two-body recombination of atomic hydrogen on $^3\text{He}-^4\text{He}$ mixture films, *Phys. Rev. Lett.* **86**, 3356 (2001).
- [34] I. Shinkoda and W. Hardy, ESR on adsorbed doubly spin-polarized atomic hydrogen, *Journal of low temperature physics* **85**, 99 (1991).
- [35] N. Pavloff and J. Treiner, ^3He impurity states on liquid ^4He : From thin films to the bulk surface, *J. Low Temp. Phys.* **83**, 331 (1995).
- [36] A. P. Mosk, M. W. Reynolds, and T. W. Hijmans, Atomic deuterium adsorbed on the surface of liquid helium, *Phys. Rev. A* **64**, 022901 (2001).
- [37] W. C. Stwalley, Simple long range model and scaling relations for the binding of isotopic hydrogen atoms to isotopic helium surfaces, *Chem. Phys. Lett.* **4**, 404 (1982).
- [38] F. O. Goodman, Effective potentials for the scattering of hydrogen and helium atoms by the surface of liquid helium, *Surface Science* **214**, 577 (1989).
- [39] K. E. Kurten and M. Ristig, Atomic and molecular hydrogen isotopes in liquid helium, *Phys. Rev. B* **31**, 1346 (1985).

- [40] M. Saarela and E. Krotscheck, Hydrogen isotope and ^3He impurities in liquid ^4He , *J. Low Temp. Phys.* **90**, 415 (1993).
- [41] M. W. Reynolds, M. E. Hayden, and W. N. Hardy, Hyperfine resonance of atomic deuterium at 1 K, *Journal of Low Temperature Physics* **84**, 87 (1991).
- [42] R. Mayer and G. Seidel, Electron-spin resonance of atomic hydrogen and deuterium at low temperatures, *Phys. Rev. B* **31**, 4199 (1985).
- [43] I. F. Silvera and J. T. M. Walraven, Spin-polarized atomic hydrogen (North-Holland, Amsterdam, 1986) p. 139.
- [44] M. G. Elliott and B. Jones, Elastic and spin-changing cross sections of spin-polarized atomic tritium, *Phys. Rev. A* **112**, 062818 (2025).
- [45] M. J. Jamieson, A. Dalgarno, and M. Kimura, Scattering lengths and effective ranges for he-he and spin-polarized h-h and d-d scattering, *Phys. Rev. A* **51**, 2626 (1995).
- [46] W. Swtalley, Collisions and reactions of ultracold molecules, *Can. J. Chem.* **82**, 709 (2004).
- [47] B. J. P. Jones, Low energy elastic scattering of H, D and T on ^3He and ^4He , arXiv **physics.atom-ph**, 2601.22360v (2026).
- [48] H. T. C. Stoof, J. M. V. A. Koelman, and B. J. Verhaar, Spin-exchange and dipole relaxation rates in atomic hydrogen: Rigorous and simplified calculations, *Phys. Rev. B* **38**, 4688 (1988).
- [49] H. F. Hess, G. P. Kochanski, J. M. Doyle, N. Masuhara, D. Kleppner, and T. J. Greytak, Magnetic trapping of spin-polarized atomic hydrogen, *Phys. Rev. Lett.* **59**, 672 (1987).
- [50] J. M. Doyle, *PhD. Thesis: Energy Distribution Measurements of Magnetically Trapped Spin-Polarized Atomic Hydrogen: Evaporative Cooling and Surface Sticking*, Ph.D. thesis, MIT (1991).
- [51] R. van Roijen, J. J. Berkhout, S. Jaakkola, and J. T. M. Walraven, Experiments with atomic hydrogen in a magnetic trapping field, *Phys. Rev. Lett.* **61**, 931 (1988).
- [52] J. M. V. A. Koelman, H. T. C. Stoof, B. J. Verhaar, and J. T. M. Walraven, Spin-polarized deuterium in magnetic traps, *Phys. Rev. B* **38**, 9319 (1988).
- [53] D. E. Pritchard, Cooling neutral atoms in a magnetic trap for precision spectroscopy, *Phys. Rev. Lett.* **51**, 1336 (1983).
- [54] H. F. Hess, Evaporative cooling of magnetically trapped and compressed spin-polarized hydrogen, *Phys. Rev. B* **34**, 3476 (1986).
- [55] J. Ahokas, A. Semakin, J. Järvinen, O. Hanski, A. Laptiyenko, V. Dvornichenko, K. Salonen, Z. Burkley, P. Crivelli, A. Golovizin, V. Nesvizhevsky, F. Nez, P. Yzombard, E. Widmann, and S. Vasiliev, A large octupole magnetic trap for research with atomic hydrogen, *Review of Scientific Instruments* **93**, 023201 (2022).
- [56] J. Ahokas, O. Vainio, J. Järvinen, V. V. Khmelenko, D. M. Lee, and S. Vasiliev, Stabilization of high-density atomic hydrogen in H_2 films at $T < 0.5$ K, *Phys. Rev. B* **79**, 220505R (2009).
- [57] M. Sharnoff and R. V. Pound, Magnetic resonance studies of unpaired atoms in solid D_2 , *Phys. Rev.* **132**, 1003 (1963).
- [58] G. W. Collins, P. C. Souers, J. L. Maienschein, E. R. Mapoles, and J. R. Gaines, Atomic-hydrogen concentrations in solid D-T and T_2 , *Phys. Rev. B* **45**, 549 (1992).
- [59] S. Sheludiakov, *PhD. Thesis: Magnetic Resonance Study of Atomic Hydrogen Stabilized in Matrices of Hydrogen Isotopes below 1K*, Ph.D. thesis, University of Turku (2017).
- [60] S. Sheludiakov, J. Ahokas, J. Järvinen, L. Lehtonen, O. Vainio, S. Vasiliev, D. M. Lee, and V. V. Khmelenko, Esr study of atomic hydrogen and tritium in solid T_2 and $\text{T}_2\text{:H}_2$ matrices below 1 K, *Phys. Chem. Chem. Phys.* **19**, 2834 (2017).
- [61] R. Jochemsen, M. Morrow, A. Berlinsky, and W. Hardy, Magnetic resonance studies of atomic hydrogen at zero field and low temperature: Recombination and binding on liquid helium, *Physica B+C* **109-110**, 2108 (1982), 16th International Conference on Low Temperature Physics, Part 3.
- [62] B. W. Statt, W. N. Hardy, A. J. Berlinsky, and E. Klein, ESR studies of spin-polarized atomic hydrogen using a 114-GHz heterodyne spectrometer, *Journal of Low Temperature Physics* **61**, 471 (1985).
- [63] R. J. Donnelly, Recommended values for the latent heat of evaporation of liquid ^4He , <https://pages.uoregon.edu/rjd/vapor17.htm>.
- [64] H. van Dijk, M. Durieux, J. R. Clement, and J. K. Logan, The “1958 He_4 scale of temperatures”: Part 2. tables for the 1958 temperature scale, *Journal of research of the National Bureau of Standards. Section A, Physics and chemistry* **64A**, 4 (1960).
- [65] W. Kaufman, T. Roser, and B. Vuaridel, Ultra-cold atomic hydrogen beam, *Nuclear Instruments and Methods in Physics Research Section A: Accelerators, Spectrometers, Detectors and Associated Equipment* **335**, 17 (1993).
- [66] R. D. McCarty, The thermodynamic properties of helium II from 0 K to the lambda transitions (1980).
- [67] Y. H. Huang and G. B. Chen, A practical vapor pressure equation for helium-3 from 0.01 k to the critical point, *Cryogenics* **46**, 833 (2006).
- [68] P. J. Nacher, M. Cornut, and M. E. Hayden, Compression of ^3He by refluxing ^4He : A model for computing hevac effects in ^3He - ^4He mixtures, *Journal of low temperature physics* **97**, 417 (1994).
- [69] P. Huffman *et al.*, Design and performance of a cryogenic apparatus for magnetically trapping ultracold neutrons, *Cryogenics* **64**, 40 (2014).
- [70] C. O’Shaughnessy *et al.*, Measuring the neutron lifetime using magnetically trapped neutrons, *Nuclear Instruments and Methods in Physics Research Section A: Accelerators, Spectrometers, Detectors and Associated Equipment* **611**, 171 (2009).
- [71] A. Ashtari Esfahani, S. Bhagyati, S. Böser, M. J. Brandsema, R. Cabral, V. A. Chirayath, C. Claessens, N. Coward, L. de Viveiros, P. J. Doe, M. G. Elliott, S. Enomoto, M. Ferti, J. A. Formaggio, B. T. Foust, J. K. Gaison, P. Harmston, K. M. Heeger, B. J. P. Jones, E. Karim, K. Kazkaz, P. T. Kolbeck, M. Li, A. Lindman, C.-Y. Liu, C. Matthé, R. Mohiuddin, B. Monreal, B. Mucogllava, R. Mueller, A. Negi, J. A. Nikkel, E. Novitski, N. S. Oblath, M. Oueslati, J. I. Peña, W. Pettus, V. S. Ranatunga, R. Reimann, A. L. Reine, R. G. H. Robertson, L. Saldaña, P. L. Slocum, F. Spanier, J. Stachurska, K. Stogsdill, Y.-H. Sun, P. T. Surukuchi, L. Taylor, A. B. Telles, F. Thomas, L. A. Thorne, T. Thümmler, W. Van De Pontseele, B. A. VanDevender, T. E. Weiss, M. Wynne, and A. Ziegler (Project 8 Collaboration), Dy-

- namics of magnetic evaporative beamline cooling for the preparation of cold atomic beams, *Phys. Rev. A* **112**, 033311 (2025).
- [72] A. C. N. Lindman, *PhD. Thesis: Atomic Tritium Technology: Production, Cooling, and Trapping for Neutrino Mass Measurement*, Ph.D. thesis, Johannes Gutenberg University, Mainz (2025).
- [73] A. Matveev, C. G. Parthey, K. Predehl, J. Alnis, A. Beyer, R. Holzwarth, T. Udem, T. Wilken, N. Kolachevsky, M. Abgrall, D. Rovera, C. Salomon, P. Laurent, G. Grosche, O. Terra, T. Legero, H. Schnatz, S. Weyers, B. Altschul, and T. W. Hänsch, Precision measurement of the hydrogen 1S–2S frequency via a 920-km fiber link, *Phys. Rev. Lett.* **110**, 230801 (2013).
- [74] K. Ishikawa *et al.*, Porous plug and superfluid helium film flow suppressor for the soft x-ray spectrometer onboard astro-h, *Cryogenics* **50**, 507 (2010).
- [75] R. Anthony-Petersen *et al.*, Demonstration of the herald superfluid helium detector concept, *Phys. Rev. D* **110**, 072006 (2024).
- [76] J. Helffrich, M. Maley, M. Krusius, and J. C. Wheatley, Hydrogen dissociation below 1 K, *Journal of Low Temperature Physics* **66**, 277 (1987).
- [77] S. D. Hogan, A. W. Wiederkehr, H. Schmutz, and F. Merkt, Magnetic trapping of hydrogen after Multistage Zeeman Deceleration, *Phys. Rev. Lett.* **101**, 143001 (2008).
- [78] R. B. Hallock, The properties of multilayer ^3He - ^4He mixture films (Elsevier Science B.V., 1995) pp. 321–443.
- [79] J. Schou and H. Sørensen, The penetration depth of 0.5–3-keV electrons in solid hydrogen and deuterium, *Journal of Applied Physics* **49**, 816 (1978).